

Article

A New Genus and Two New Species of Fireflies from South America (Lampyridae: Lampyrinae: Photinini) [†]

André Silva Roza ^{1,*} , José Ricardo Miras Mermudes ¹  and Luiz Felipe Lima da Silveira ²

¹ Laboratório de Entomologia, Departamento de Zoologia, Instituto de Biologia, Universidade Federal do Rio de Janeiro, A1-107, Bloco A, Av. Carlos Chagas Filho, Cidade Universitária, Ilha do Fundão, Rio de Janeiro 373, Brazil

² Biology Department, Western Carolina University, 1 University Drive, Cullowhee, NC 28723, USA

* Correspondence: andreroza1993@gmail.com

† Zoobank LSID: Zoiudo: urn:lsid:zoobank.org:act:8D57236E-C76F-4A6A-83B8-F95A3E0A0AA9; Zoiudo araucariorum: urn:lsid:zoobank.org:act:3250C749-CBE8-4CE1-928A-377C58E32001; Zoiudo rosae: urn:lsid:zoobank.org:act:EA686303-3D49-49A4-8DDB-58DC4B4A2B4B.

Abstract: Lampyridae taxonomy has traditionally relied on a few characters now deemed to be highly homoplastic, and their classification—especially at the genus level—is yet to be consolidated based on rigorous phylogenetic analyses. Recent studies highlighted the value of genitalic trait variation in the evolution in Lampyridae, particularly for the rich and poorly known South American Photinini fauna. Here, we describe a new genus, with a new species from the Cerrado and another one from the Atlantic Forest. Phylogenetic analyses based on Bayesian and Maximum Parsimony approaches recovered these two species as sister to each other, which we place here in *Zoiudo* gen. nov. Males of this new lineage of fireflies are overall strikingly similar to *Photinus* Laporte 1833, but can be readily distinguished by traits heretofore neglected, including the structure of tibial spurs and many genitalic traits. Instead, *Zoiudo* gen. nov. is strongly supported as sister to *Ybytyramoan* Silveira and Mermudes, 2014, supported by eight synapomorphies, the most conspicuous being the sternum VIII with lateral margins divergent up to basal 1/5, then convergent posteriorly, and the rudimentary ventral plate of phallus. Our study confirms the value of extensive character and taxon sampling towards a revised classification of Photinini taxa and highlights the need for a continued sampling and protection of South American biomes.

Keywords: Atlantic Forest; Cerrado; Neotropical region; *Photinus*; phylogeny; *Ybytyramoan*; *Zoiudo*



Citation: Roza, A.S.; Mermudes, J.R.M.; Silveira, L.F.L.d. A New Genus and Two New Species of Fireflies from South America (Lampyridae: Lampyrinae: Photinini). *Diversity* **2022**, *14*, 1005. <https://doi.org/10.3390/d14111005>

Academic Editors: Michael Wink and Andrey Frolov

Received: 17 October 2022

Accepted: 17 November 2022

Published: 19 November 2022

Publisher's Note: MDPI stays neutral with regard to jurisdictional claims in published maps and institutional affiliations.



Copyright: © 2022 by the authors. Licensee MDPI, Basel, Switzerland. This article is an open access article distributed under the terms and conditions of the Creative Commons Attribution (CC BY) license (<https://creativecommons.org/licenses/by/4.0/>).

1. Introduction

Fireflies (Coleoptera: Lampyridae) are a charismatic group of beetles with a surprisingly confused taxonomy. Lampyridae taxonomy—especially at the genus-level—is traditionally reliant on few characters recurrently shown to be homoplastic (e.g., [1–5]), which complicates their classification and identification. Most genera of fireflies across subfamilies were last comprehensively reviewed over a century ago, and their diagnoses must be updated upon a phylogenetic framework.

Photinini LeConte, 1881, is the largest Lampyrinae tribe, with around 750 species and over 30 genera [6,7]. Despite the description of several new genera and species (e.g., [8–10]), many taxa in this tribe are difficult to identify due to overlapping genus-level diagnoses in this tribe. Recent phylogenetic studies have highlighted the value of previously overlooked morphological characters, mainly in the male terminalia and genitalia, to unravel the evolution and relationship of Photinini taxa [2,4,5]. The study and phylogenetic assessment of these characters has helped to improve and stabilize the tribe's classification, benefiting both taxonomists and non-taxonomists.

More than half of the world's Lampyridae (ca 2200 species) are housed in the Neotropics [11]. In the Neotropical realm, the South American fauna stands out due to its high

diversity and endemism [11]. Much of this diversity is, however, known only by their original descriptions and illustrations, which are usually insufficient to inform identification (e.g., [6]). Past work on the firefly fauna of the Atlantic Forest (e.g., [4]) and, more recently, Amazonia (e.g., [5]), led to the discovery of dozens of new species, but most other South American biomes remain unexplored, with their firefly fauna almost completely unknown. The Cerrado stands out as one of the most species-rich South American biomes, with a high level of endemism [12]. This biome is highly threatened by human activities, with 55% of its area already deforested [13]. Sadly, most of its firefly fauna remain unstudied and many taxa unknown to science may be extinct even before their description.

Recent examination of museum entomological collections allowed us to identify two undescribed species—one from Cerrado and other from an unexplored area of the Atlantic Forest—which resemble *Photinus* Laporte, 1833 and *Ybytyramoan* Silveira and Mermudes, 2014. In order to explore the phylogenetic relationships of these two new species and improve the standing diagnoses of Photinini genera, we performed a phylogenetic analysis including most of the tribe genera. Our phylogenetic analyses based on Bayesian and maximum parsimony criteria recovered these two new species as sisters to each other, in a new genus described and illustrated herein.

2. Materials and Methods

2.1. Morphology, Terminology, and Illustrations

We examined specimens from the following institutions: Museu de Zoologia da Universidade de São Paulo, São Paulo, Brazil (MZUSP); Coleção de Entomologia Prof. José Alfredo Pinheiro Dutra, Universidade Federal do Rio de Janeiro, Rio de Janeiro, Brazil (DZRJ); and the Seção de Entomologia da Coleção Zoológica, Universidade Federal do Mato Grosso, Mato Grosso, Brazil (CEMT). Whole specimens or only their dissected abdomens were soaked in 10% KOH for 24–48 h. Photographs were made with a Leica DFC5400 and Leica Application Suite CV3 multi-focus software or with a Leica M205 C stereomicroscope and Leica Application Suite X Automontage Software.

We recorded label data for all type specimens using the following conventions: double quotes (“ ”) for label data quoted verbatim, single forward slashes to separate label lines (/), double backslashes (\\) to separate labels; and brackets [] to enclose our comments or notes. All labels are typed unless otherwise noted.

The classification follows [14] and terminology follows [9], except for wing terminology, which follows [15]. A distribution map of the species was plotted on the biogeographical map of the Neotropical region provided in [16] using R packages “sf”, “dplyr”, and “ggplot2”.

2.2. Taxon Sampling

The new genus, with the two new species, could be confidently placed in Photinini based on their morphology. To determine the placement of the two new species, we expanded the taxon sampling of [7], which included taxa from all four Photinini subtribes, by adding the two new species and two *Ybytyramoan* Silveira and Mermudes, 2017 species (total = 25 species). Data for the material examined of the new species in the new genus are provided below (see Results), and additional material used in the phylogenetic analyses is provided in Supplementary Material S1. The root was set on the *Lampyris noctiluca* (Linnaeus, 1758) (Lampyridae: Lampyrini), which was never placed in Photinini. However, we also tested on the other non-Photinini taxon, *Vesta thoracica* (Olivier, 1790) (Lampyridae: Incertae sedis).

2.3. Phylogenetic Analysis

Our matrix expanded on the 93 morphological characters listed in [7], by adding four new characters (total = 97). Character coding followed the logical basis of [17]. The matrix was constructed in Mesquite v3.2 [18]. The character matrix is provided in Supplementary

Material S2. The proposition of homologies was based on direct observations of adult males and females.

We ran phylogenetic analyses based on maximum parsimony (MP) and Bayesian inference (BI). We ran the MP analyses on TNT [19], using new technology heuristic searches with tree bisection and reconnection, with equal and implied weights (EW and IW, respectively), unevenly scaling the k parameter to investigate how homoplasy impacts tree topology [20,21]. Node support was assessed using the Bremer index (for MP–EW) and symmetric resampling (for both MP–EW and MP–IW) with 1000 replicates.

BI was run in MrBayes 3.2.7a [22] (available at The CIPRES Science Gateway V. 3.3 (<https://www.phylo.org/portal2/login!input.action>, accessed on 13 September 2022)–[23]). A model selection ran with ModelFinder [24] in IQ-TREE2 [25] selected the MKV model [26] with equal state frequencies, 4 gamma categories, and correction for ascertainment bias (i.e., MK+FQ+ASC+G4) (Supplementary Material S3). We ran 10×10^6 generations, saving trees every 2000 generations and discarding the first 25% as burn-in. We checked for convergence using Tracer v1.6 [27]. Character evolution was optimized on the Bayesian majority consensus tree using WinClada [28].

Trees were read in FigTree version 1.4.4 (obtained at <https://github.com/rambaut/figtree/releases>; accessed on 2 January 2021) and edited on Adobe Photoshop 2022.

3. Results

3.1. Characters

Our matrix included 97 characters from male and female specimens, spanning the three tagmata: head (10), thorax (19), and abdomen (68, 41 of which from the aedeagus). For each character, the following is indicated for the MP–EW analysis: the number of steps (L); the consistency index (CI); and the retention index (RI).

1. Antenna, antennomeres III–IX, core, shape: (0) serrate; (1) cylindrical (Figure 4F). L = 6; CI = 16; RI = 16.
2. Antenna, antennomeres III–IX, single lamellae: (0) absent (Figure 4F); (1) present (branch longer than core antennomere). L = 3; CI = 33; RI = 0.
3. Clypeus, connection to frons: (0) connected by membrane throughout (Figure 4D); (1) completely obliterate; (2) connate by median third. L = 3; CI = 66; RI = 75.
4. Mandibles, orientation in frontal view: (0) overlapping (Figure 4D); (1) crossed (Supplementary Material Figure S4A); (2) convergent (Supplementary Material Figure S4C). L = 2; CI = 100; RI = 100.
5. Mandible, apex, shape: (0) sharp (Figure 4A); (1) blunt (Supplementary Material S4B); (2) rounded (Supplementary Material S4C). L = 3; CI = 66; RI = 80.
6. Mandible, curvature: (0) straight (Supplementary Material Figure S4C); (1) evenly curved (Supplementary Material S4B); (2) almost right-angled (basal half straight, Figure 4C). L = 2; CI = 100; RI = 100.
7. Labrum, sclerite, anterior margin, shape: (0) straight; (1) emarginate (Figure 4A). L = 5; CI = 20; RI = 63.
8. Labium, submentum, anterior margin, shape: (0) straight (Figure 4B); (1) notched. L = 1; CI = 100; RI = 100.
9. Labium, submentum, lateral margins, shape: (0) subparallel to slightly convergent posteriorly; (1) abruptly constrained posteriorly; (2) strongly convergent posteriorly (Figure 4B). L = 8; CI = 25; RI = 45.
10. Labium, palp, palpomere III, lateral margins, shape: (0) obconical; (1) subparallel; (2) divergent apically (Figure 4B). L = 3; CI = 66; RI = 50.
11. Pronotum, anterior margin, shape: (0) acuminate anteriorly; (1) evenly rounded (Figure 5B). L = 4; CI = 25; RI = 40.
12. Pronotum (lateral view), anterior expansion, curvature: (0) curved upwards; (1) straight (Figure 5E). L = 1; CI = 100; RI = 100.
13. Pronotum, lateral margin, length relative to disc: (0) less than a third (Figure 5E); (1) nearly half; (2) at least 1. L = 4; CI = 25; RI = 50.

14. Pronotum, disc, sagittal depression: (0) absent (Figure 5A); (1) present. L = 1; CI = 100; RI = 100.
15. Pronotum, by the disc, posterior margin, shape: (0) strongly sinuose; (1) almost straight; (2) slightly emarginate (Figure 5A). L = 2; CI = 100; RI = 100.
16. Pronotum, posterior corner, notch, presence: (0) absent (Figure 5A); (1) present. L = 5; CI = 20; RI = 50.
17. Hypomeron (lateral view), ratio between hypomeron depth and pronotal lateral expansion width: (0) about as long (Figure 5E); (1) at least a 1/5 shorter; (2) at least a 1/5 longer. L = 5; CI = 40; RI = 50.
18. Hypomeron (ventral view), area anterior to prosternal insertior, shape: (0) projecting outwards; (1) straight (Figure 5B). L = 1; CI = 100; RI = 100.
19. Prosternum, anterior margin, shape: (0) medially sinuose; (1) straight (Figure 5B). L = 5; CI = 20; RI = 50.
20. Mesoscutellum, posterior margin, shape: (0) rounded; (1) truncate (Figure 5F). L = 5; CI = 20; RI = 42.
21. Elytron, outer margin, shape: (0) straight; (1) rounded; (2) convergent posteriorly (Figure 5L); (3) widest at apical third. L = 7; CI = 42; RI = 50.
22. Wing, position of MP3+4 split, relative to CuA1: (0) more basal; (1) more apical (Figure 5M). L = 4; CI = 25; RI = 57.
23. Wing, AA3, shape: (0) short (almost as long as wide) and almost perpendicular to AA4; (1) elongate and with an acute angle to AA4 (Figure 5M). L = 3; CI = 33; RI = 60.
24. Wing, r3: (0) absent; (1) present (Figure 5M). L = 2; CI = 50; RI = 50.
25. Proleg, anterior claw, tooth: (0) absent (Figure 5N); (1) present. L = 3; CI = 33; RI = 33.
26. Proleg, tibial spurs, count: (0) zero (Figure 5N); (1) one; (2) two. L = 9; CI = 22; RI = 46.
27. Mesoleg, anterior claw, tooth: (0) absent (Figure 5N); (1) present. L = 3; CI = 33; RI = 33.
28. Mesoleg, tibial spurs, count: (0) zero (Figure 5N); (1) one; (2) two. L = 7; CI = 28; RI = 37.
29. Metaleg, tibial spurs, count: (0) zero (Figure 5N); (1) one; (2) two. L = 7; CI = 28; RI = 37.
30. Tergum I, laterotergite, shape: (0) triangular; (1) quadrangular (Figure 6A). L = 1; CI = 100; RI = 100.
31. Tergum I, spiracle, shape: (0) reniform (Figure 6A); (1) subcircular. L = 1; CI = 100; RI = 100.
32. Tergum VII, posterior angles, shape: (0) projected, embracing anterior angles of pygidium; (1) rudimentary, slightly projected backwards (Figure 6A). L = 1; CI = 100; RI = 100.
33. Sterna II-VIII, width variation: (0) progressively narrow (Figure 6B); (1) widest by sterna III-IV; (2) widest by sternum V. L = 3; CI = 66; RI = 66.
34. Sternum VI, lantern: (0) absent; (1) present (Figure 6B). L = 5; CI = 20; RI = 55.
35. Sternum VII, lantern: (0) absent; (1) present (Figure 6B). L = 3; CI = 33; RI = 71.
36. Sternum VIII, length relative to VII: (0) as long as (Figure 6B); (1) slightly longer; (2) at least a fifth shorter; (3) 2x as long; (4) at least 3x longer. L = 4; CI = 50; RI = 71.
37. Sternum VIII, lateral margins, shape: (0) rounded; (1) divergent up to basal 1/4, then convergent posteriorly (Figure 6B). L = 2; CI = 50; RI = 80.
38. Sternum VIII, posterior margin, shape: (0) almost straight (Figure 6B); (1) sinuose; (2) emarginate; (4) emarginate with a tiny mucronate projection. L = 6; CI = 33; RI = 55.
39. Sternum VIII, posterior margin, median projection: (0) absent (Figure 6B); (1) present. L = 6; CI = 16; RI = 37.
40. Sternum VIII, posterior margin, median projection, shape: (0) tiny; (1) elongate; (2) wide, triangular. L = 2; CI = 100; RI = 100.
41. Pygidium, relation between length and width: (0) at least a fifth wider than long; (1) as long as wide (Figure 6C); (2) at least a fifth longer than wide. L = 6; CI = 33; RI = 66.

42. Pygidium, lateral margins, shape: (0) subparallel; (1) rounded (Figure 6C); (2) divergent posteriorly; (3) convergent posteriorly. L = 3; CI = 100; RI = 100.
43. Pygidium, posterior margin, central third, shape: (0) almost straight; (1) rounded (Figure 6C); (2) emarginate; (3) medially notched. L = 6; CI = 50; RI = 25.
44. Pygidium, posterolateral corners, degree of development: (0) well-developed; (1) barely conspicuous (Figure 6C). L = 6; CI = 16; RI = 50.
45. Pygidium, posterolateral corners, length relative to central third: (0) shorter (Figure 6C); (1) as long as; (2) longer. L = 9; CI = 22; RI = 12.
46. Syntergite, shape (proportion): (0) longer than wide (Figure 6D); (1) wider than long. L = 4; CI = 25; RI = 0.
47. Syntergite, lateral margin, shape: (0) convergent posteriorly (Figure 6D); (1) subparallel. L = 2; CI = 50; RI = 66.
48. Syntergite, anterior margin, shape: (0) mildly emarginated (Figure 6D); (1) strongly indented; (2) almost straight. L = 3; CI = 66; RI = 75.
49. Syntergite, pattern of sclerotization: (0) evenly sclerotized (Figure 6D); (1) completely divided by a membranous line. L = 1; CI = 100; RI = 100.
50. Syntergite, length relative to sternum IX: (0) 1/3; (1) 1/2 (Figure 6D); (2) 2/3; (3) 1/5. L = 7; CI = 42; RI = 20.
51. Syntergite, posterolateral corners, chaetotaxy: (0) glabrous; (1) covered in setae; (2) with dome-shaped sensillae (Figure 6D). L = 8; CI = 25; RI = 53.
52. Sternum IX, lateral rods, shape: (0) biconcave (Figure 6D); (1) evenly convergent (Figure 6D); (2) abruptly convergent. L = 2; CI = 100; RI = 100.
53. Sternum IX, lateral rods, tips, connection: (0) separated (Figure 6D); (1) fused. L = 5; CI = 20; RI = 42. L = 4; CI = 25; RI = 57.
54. Sternum IX, length relative to aedeagus (including phallobase): (0) slightly shorter; (1) slightly longer (Figure 6D); (2) 1/3 longer. L = 6; CI = 50; RI = 72.
55. Sternum IX, position relative to VIII: (0) completely covered; (1) partially exposed (Figure 6D). L = 1; CI = 100; RI = 100.
56. Sternum IX, posterior half, degree of excavation: (0) evenly sclerotized (Figure 6D); (1) completely membranous; (2) emarginated; (3) deeply clefted (to at least a fifth sternum length). L = 2; CI = 50; RI = 50.
57. Phallobase, bilateral symmetry: (0) symmetrical; (1) asymmetrical (Figure 6E). L = 3; CI = 33; RI = 33.
58. Phallobase, length relative to phallus: (0) at least a fourth shorter (Figure 6E); (1) as long as; (2) at least a fourth longer. L = 6; CI = 33; RI = 42.
59. Phallobase, sagittal line: (0) absent (Figure 6E); (1) present. L = 5; CI = 20; RI = 60.
60. Phallobase, sagittal line, extension: (0) throughout phallobase; (1) not reaching apical margin. L = 3; CI = 33; RI = 50.
61. Phallobase, apical margin, shape: (0) slightly emarginate; (1) deeply emarginate (C-shaped, Figure 6E-I); (2) medially clefted. L = 8; CI = 25; RI = 33.
62. Phallus, dorsal plate, median connection to parameres: (0) connected by membrane (Figure 6E-I); (1) connate; (2) fused. L = 2; CI = 100; RI = 100.
63. Phallus, dorsal plate, base, pattern of sclerotization: (0) evenly sclerotized (Figure 6E-I); (1) widely membranous. L = 1; CI = 100; RI = 100.
64. Phallus, struts, condition: (0) absent (Figure 6E-I); (1) present (visible through the phallobase). L = 2; CI = 50; RI = 88.
65. Phallus, dorsal plate, ventrobasal processes, presence: (0) absent (Figure 6E-I); (1) present. L = 1; CI = 100; RI = 100.
66. Phallus, dorsal plate, ventrobasal processes, shape: (0) wider than long; (1) globose. L = 1; CI = 100; RI = 100.
67. Phallus, dorsal plate, ventrobasal processes, shape (in apical view): (0) divergent; (1) onvergent. L = 1; CI = 100; RI = 100.
68. Phallus, dorsal plate, subclef transverse groove: (0) absent (Figure 6E-I); (1) present. L = 1; CI = 100; RI = 100.

69. Phallus, dorsal plate, length relative to parameres: (0) nearly a fifth longer; (1) at least a fifth shorter; (2) as long as (Figure 6E–I); (3) twice as long. L = 7; CI = 42; RI = 50.
70. Phallus, dorsal plate, condition: (0) entire (Figure 6E–I); (1) medially split. L = 1; CI = 100; RI = 100.
71. Phallus (dorsal view), dorsal plate, anterior margin, shape: (0) rounded (Figure 6E–I); (1) pointed; (2) truncate; (3) clefted. L = 5; CI = 60; RI = 71.
72. Phallus, dorsal plate, degree of medial indentation: (0) nearly a 1/3 plate length; (1) nearly 1/2 plate length; (2) nearly 2/3 plate length; (3) completely divided; (4) slightly emarginate. L = 2; CI = 50; RI = 75.
73. Phallus, dorsal plate, apical arms (of indented Phallus), shape: (0) widely distanced and slightly convergent; (1) contiguous; (2) fused; (3) apically divergent. L = 7; CI = 42; RI = 20.
74. Phallus (lateral view), dorsal plate, overall shape: (0) straight; (1) bent dorsally; (2) slightly curved ventrally (Figure 6E–I); (3) sinuose; (4) with a basal acute angle. L = 6; CI = 50; RI = 72.
75. Phallus, dorsal plate, basal abrupt constriction: (0) absent (Figure 6E–I); (1) present. L = 1; CI = 100; RI = 100.
76. Phallus, dorsal plate, subapical outer teeth: (0) absent; (1) present (Figure 6E–I). L = 3; CI = 33; RI = 66.
77. Phallus, dorsal plate, basal joint: (0) absent (Figure 6E–I); (1) present. L = 1; CI = 100; RI = 100.
78. Phallus, dorsal plate, sides, texture: (0) smooth (Figure 6E–I); (1) toothed. L = 1; CI = 100; RI = 100.
79. Phallus, dorsal plate, longitudinal window: (0) absent (Figure 6E–I); (1) present. L = 1; CI = 100; RI = 100.
80. Phallus, dorsal plate, subapical keel: (0) absent (Figure 6E–I); (1) present. L = 2; CI = 50; RI = 66.
81. Phallus, dorsal plate, subapical keel, extent: (0) entire; (1) medially interrupted. L = 1; CI = 100; RI = 100.
82. Phallus, dorsal plate, lateral keel: (0) absent; (1) present (Figure 6E–I). L = 1; CI = 100; RI = 100.
83. Phallus, ventral plate: (0) absent; (1) present (Figure 6E–I). L = 4; CI = 25; RI = 72.
84. Phallus, ventral plate, length relative to dorsal plate: (0) half as long; (1) as long as or slightly longer; (2) a third shorter; (3) rudimentary (less than a fifth) (Figure 6E–I). L = 4; CI = 75; RI = 80.
85. Phallus, endossac opening relative to the apex of dorsal plate: (0) at it; (1) a 1/5 beyond it (Figure 6E–I). L = 5; CI = 60; RI = 80.
86. Phallus, endossac, opening, shape: (0) cylindrical (Figure 6E–I); (1) cul-de-sac. L = 1; CI = 100; RI = 100.
87. Base of paramere, basal projection: (0) absent (Figure 6E–I); (1) present. L = 1; CI = 100; RI = 100.
88. Paramere, subapical ventral spike, presence: (0) absent; (1) present (Figure 6E–I). L = 4; CI = 25; RI = 62.
89. Paramere, subapical ventral spike, shape: (0) pointy (Figure 6E–I); (1) elongate. L = 1; CI = 100; RI = 100.
90. Paramere, subapical membranous appendage: (0) absent (Figure 6E–I); (1) present. L = 1; CI = 100; RI = 100.
91. Paramere, apex (tip), curvature in lateral view: (0) straight; (1) slightly curved ventrally (Figure 6E–I); (2) evenly curved inwards; (3) curved dorsally; (4) embracing phallus ventrally; (5) sinuose, curved inwards; (6) strongly curved dorsal. L = 6; CI = 66; RI = 80.
92. Paramere, apex (tip), sclerotization relative to core paramere: (0) as sclerotized; (1) distinctly membranous (Figure 6E–I); (2) more sclerotized (darker). L = 6; CI = 16; RI = 50.

93. Paramere, apex (tip), shape: (0) rounded; (1) blunt (Figure 6E–I); (2) pointed; (3) truncated. L = 4; CI = 50; RI = 71.
94. Paramere (lateral view), basal lobe: (0) absent; (1) present (Figure 6E–I). L = 2; CI = 50; RI = 90.
95. Paramere (lateral view), basal lobe, shape: (0) robust, rounded (Figure 6E–I); (1) narrow and acute; (2) rudimentary. L = 2; CI = 100; RI = 100.
96. Paramere, inner face, shape: (0) smooth (Figure 6E–I); (1) excavate. L = 3; CI = 33; RI = 33.
97. Paramere, base, orientation relative to phallus: (0) dorsal; (1) lateral (coplanar) (Figure 6E–I); (2) ventral. L = 4; CI = 25; RI = 72.

3.2. Phylogenetic Analyses

Maximum parsimony (MP) applied with equal weights found three most parsimonious trees (L = 339; CI = 43; RI = 60), which were largely congruent with the Bayesian inference (BI) majority consensus (Figure 1; Supplementary Material S5). Rooting the tree on *Vesta thoracica* (Lampyridae: Incertae sedis) did not cause any different phylogenetic interpretation. Conflicts in the topologies were found only at relatively deeper nodes and varied across the range of k values investigated (Supplementary Material S5). Both approaches recovered *Zoiudo* gen. nov. as monophyletic with high support, with six synapomorphies on its branch (Figure 2): posterior margin of pronotum slightly emarginated (15:2, not homoplastic), posterior margin of mesoscutellum truncate (20:1, homoplastic), mesoleg (28:0, homoplastic) and metaleg (29:0, homoplastic) lacking tibial spurs, anterior margin of the dorsal plate of phallus rounded (71:0, homoplastic), and lateral keels on the dorsal plate present (82:1, not homoplastic).

Zoiudo gen. nov. was consistently recovered with high support as sister to *Ybytyramoan* (Figure 1, Supplementary Material S5). This relationship is supported by eight synapomorphies (seven homoplastic), the most conspicuous ones being the sternum VIII with lateral margins convergent posteriorly (36:1, homoplastic), and the rudimentary ventral plate of phallus (83:3, not homoplastic). *Ybytyramoan* monophyly was recovered with moderate support in MP (both EW and IW) but with poor support in BI. The latter genus was supported by three homoplastic synapomorphies (Figure 2). *Lucidota banoni* Laporte, 1833 was consistently found sister to *Ybytyramoan* + *Zoiudo*, with moderate support, in all analyses (except the EW, which recovered this node in a polytomy). The most remarkable synapomorphy of *Lucidota banoni* with (*Ybytyramoan* + *Zoiudo*) is the blunt apex of the mandible. Overall, the backbone of Photinini was poorly resolved in all analyses (Figure 1, Supplementary Material S5). When topologies were found with finer resolution on the implied weights maximum parsimony analyses, the nodes were overall poorly supported (Supplementary Material S5).

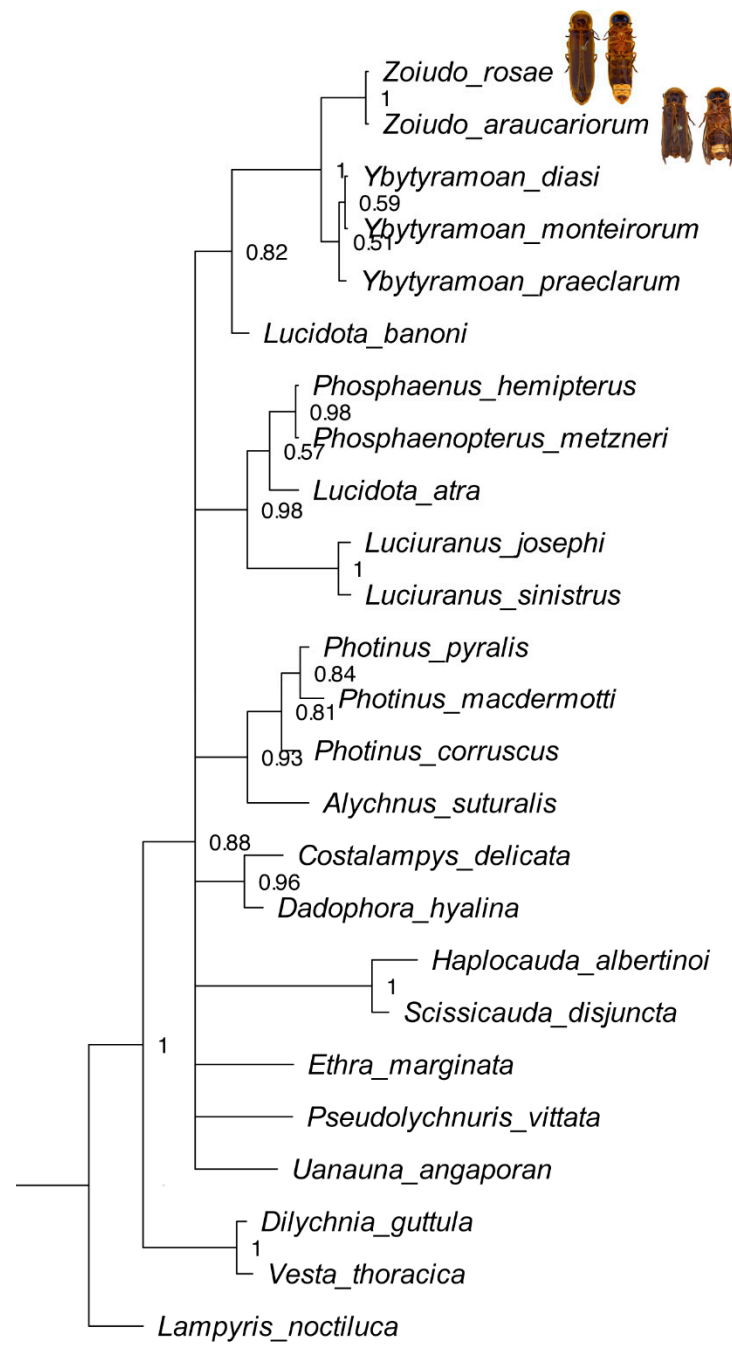


Figure 1. Majority rule Bayesian consensus tree of 97 morphological characters of 25 taxa, with dorsal habiti of the two new *Zoiudo* species plotted after their names.

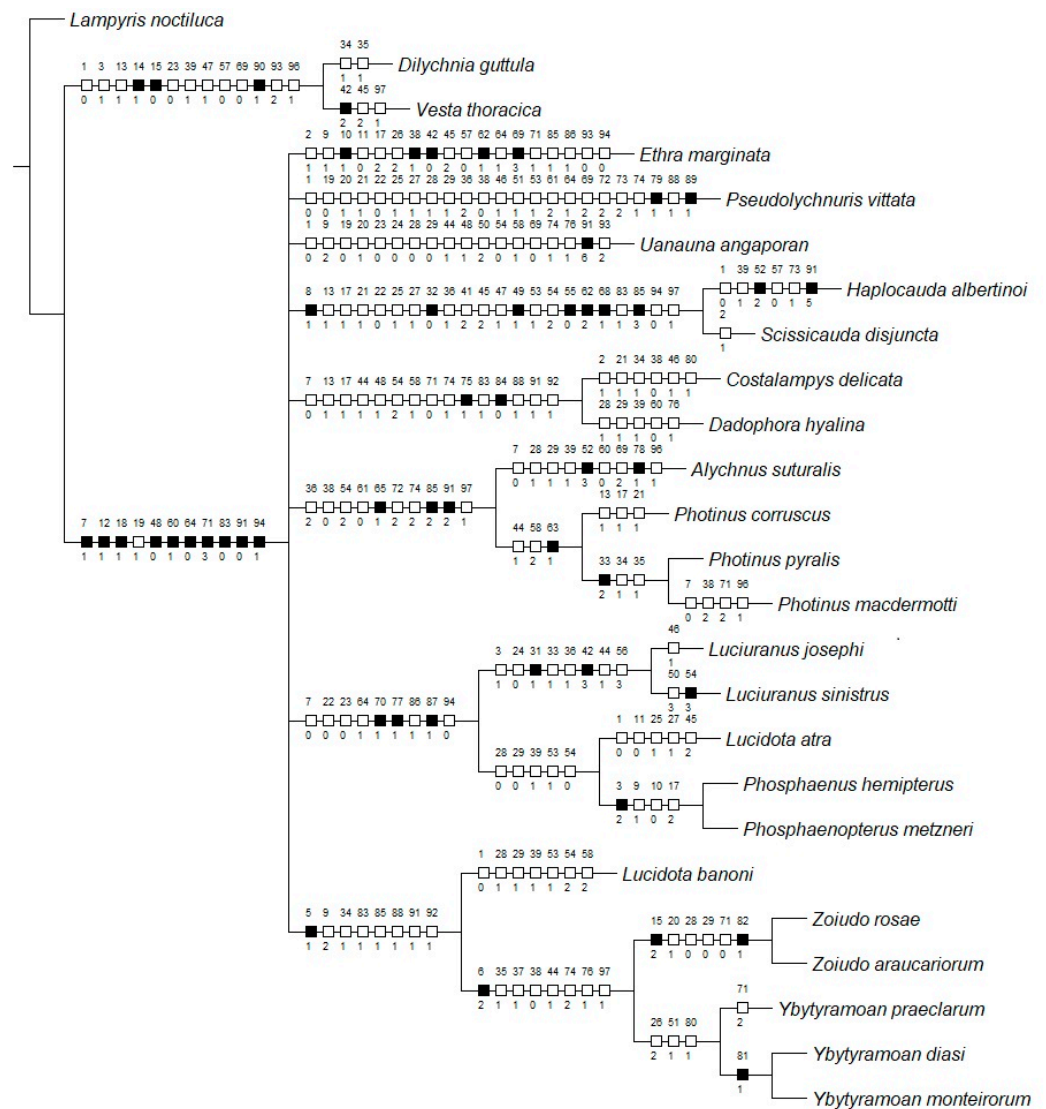


Figure 2. Maximum parsimony optimization of character state changes plotted on the majority rule Bayesian consensus tree. Black squares represent non-homoplastic synapomorphies. White squares represent homoplastic synapomorphies.

3.3. Taxonomy

Elateroidea Leach, 1815

Lampyridae Rafinesque, 1815

Lampyrinae Rafinesque, 1815

Photinini Olivier, 1907

***Zoiudo* Roza, Mermudes and Silveira gen. nov.**

(Figure 3, Figure 4, Figure 5, Figure 6, Figure 7, Figure 8, Figure 9)

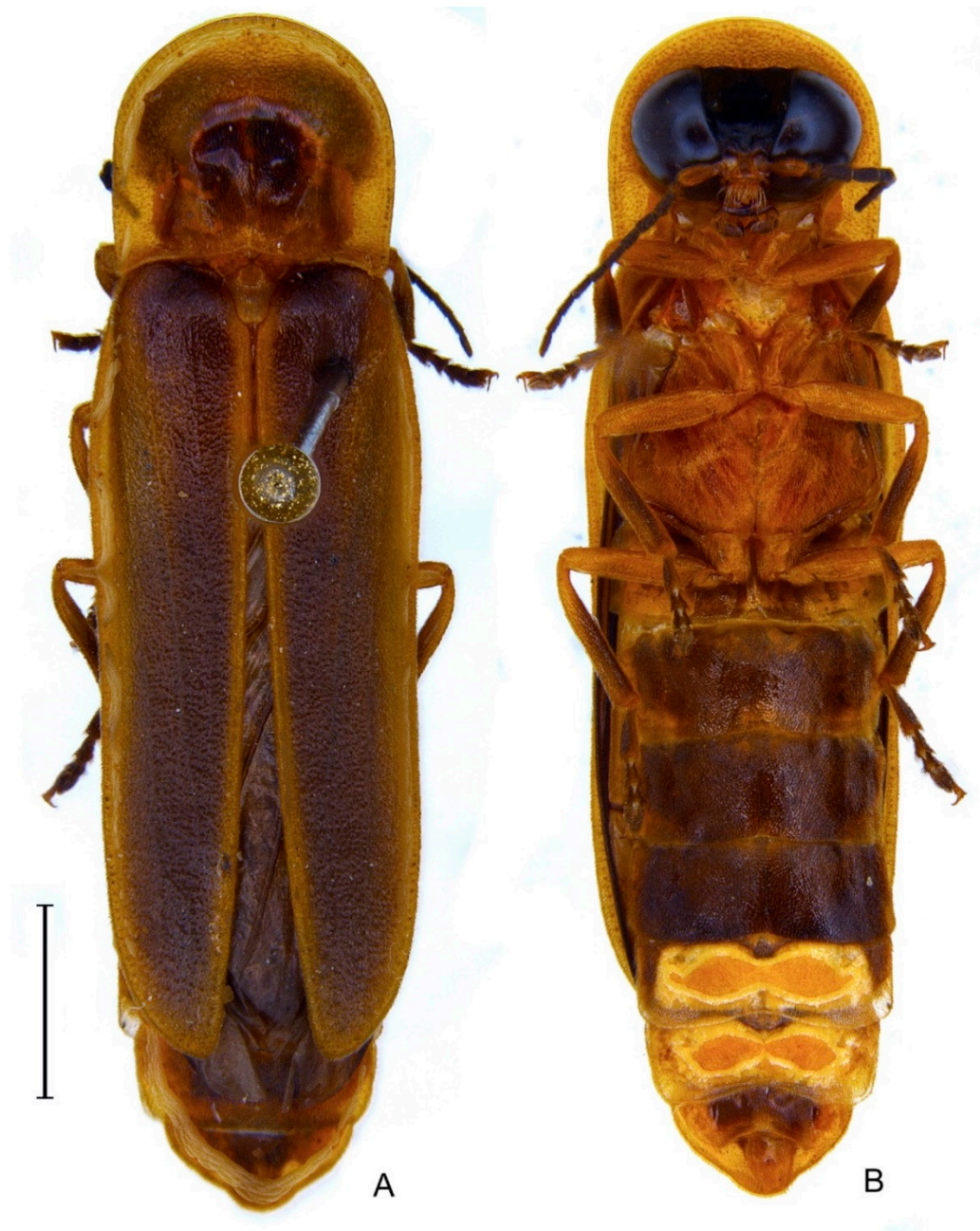


Figure 3. *Zoiudo rosae* sp. nov., habitus (A) dorsal, (B) ventral. Scale bar: 3 mm.

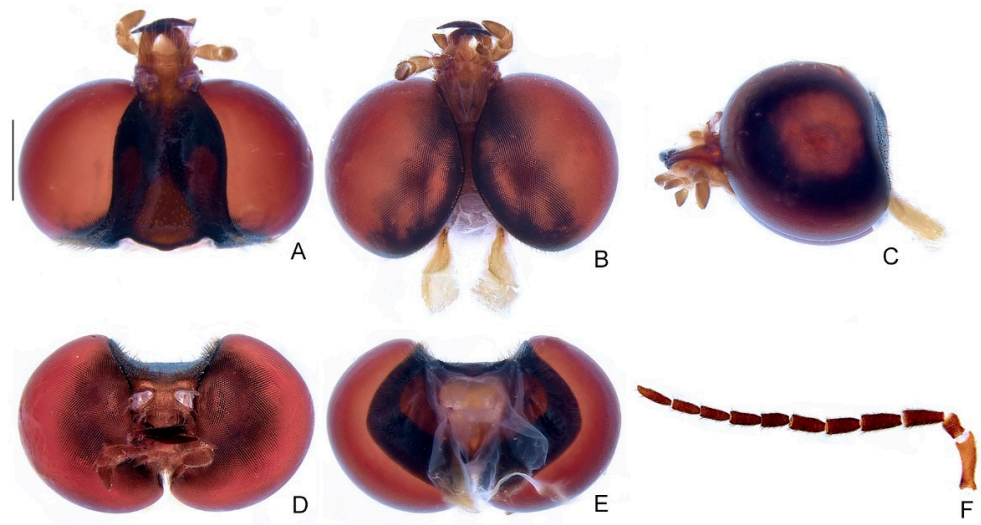


Figure 4. *Zoiudo rosae* sp. nov., head. (A–E) Head capsule: (A) dorsal, (B) ventral, (C) lateral, (D) frontal, (E) posterior. (F) Antenna, lateral. Scale bar: 1 mm.

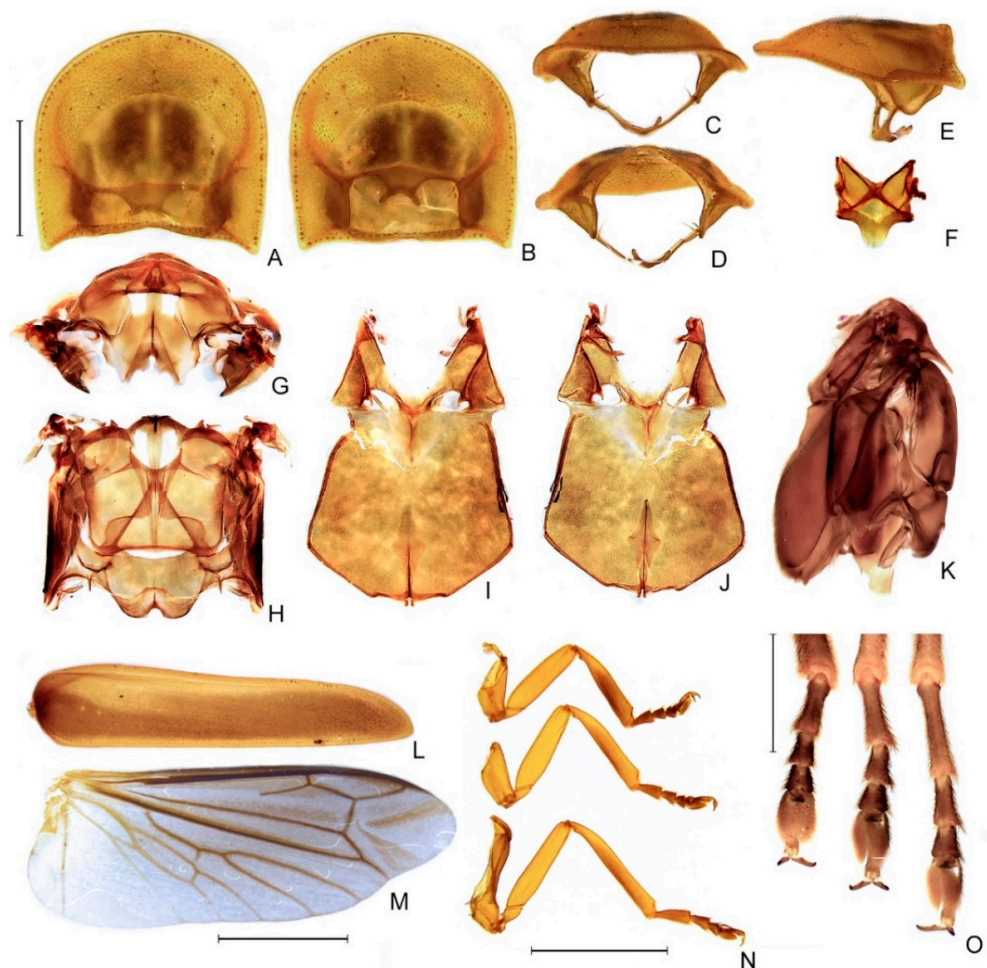


Figure 5. *Zoiudo rosae* sp. nov., thorax. (A–E) Pronotum: (A) dorsal, (B) ventral, (C) frontal, (D) posterior, (E) lateral. (F) Metascutellum, dorsal. (G) Metanotum, anterior. (H) Metanotum, dorsal. (I–K) Pterothorax: (I) ventral, (J) dorsal, (K) lateral. (L) Right elytron, dorsal. (M) Right wing, dorsal. (N) Pro-, meso-, and metaleg, from top to bottom, respectively. (O) Pro-, meso- and metatarsus, from left to right, ventral. Scale bar: A–K: 2 mm.

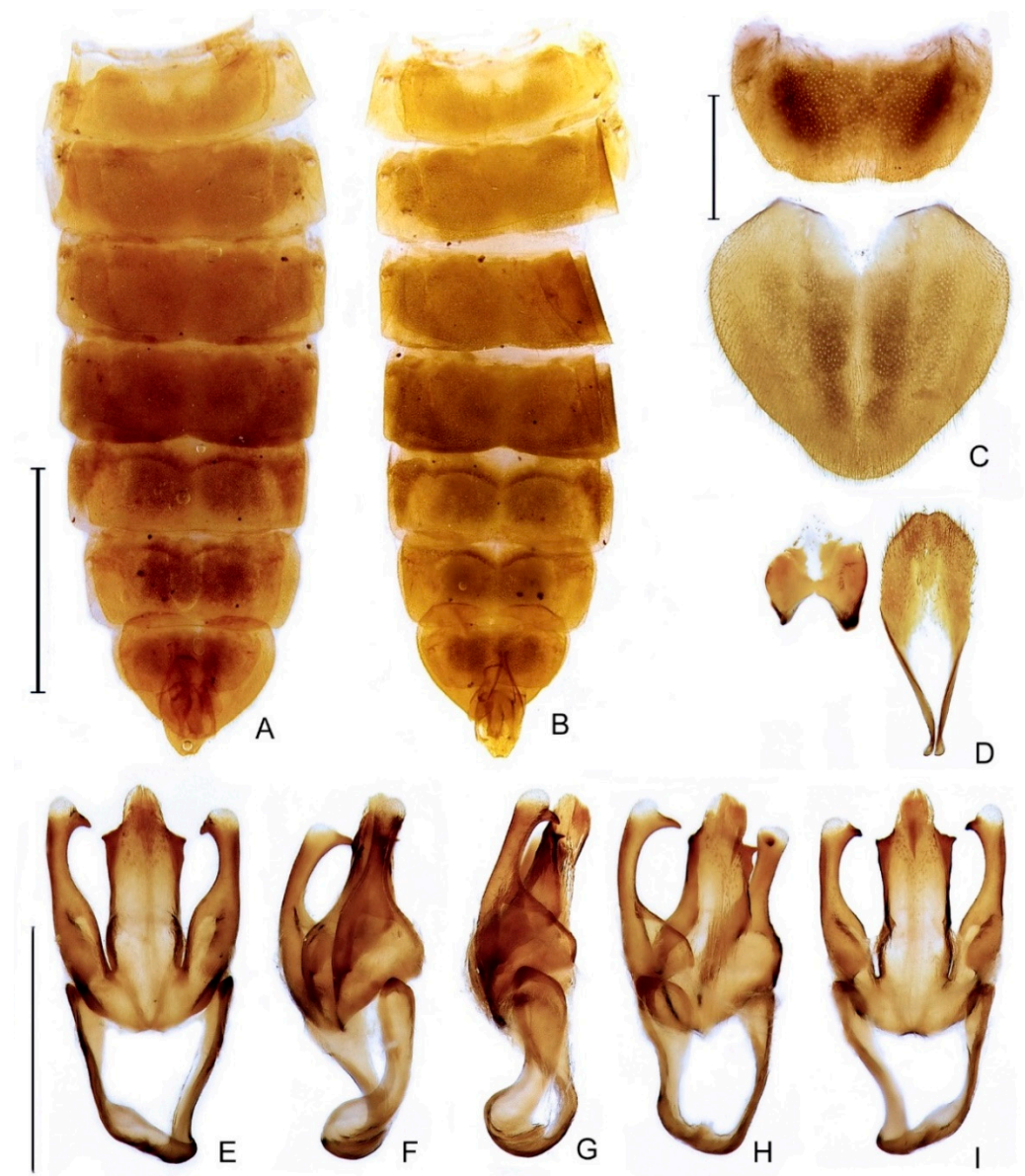


Figure 6. *Zoiudo rosae* sp. nov., abdomen. (A,B) General morphology: (A) dorsal, (B) ventral. (C) Pygidium, dorsal, and sternum VIII, ventral. (D) Aedeagal sheath (syntergite, dorsal; sternum IX, ventral). Aedeagus (E–I): (E) dorsal, (F) dorsolateral, (G) lateral, (H) lateroventral, (I) ventral. Scale bars: (A,B): 4 mm; (C,D): 1 mm; (E–I): 1 mm.



Figure 7. *Zoiudo araucariorum* sp. nov., habitus (A) dorsal, (B) ventral. Scale bar: 5 mm.



Figure 8. *Zoiudo araucariorum* sp. nov., (A) pronotum, dorsal. (B) Head, frontal. (C) Head and prothorax, lateral. Scale bar: 2 mm.

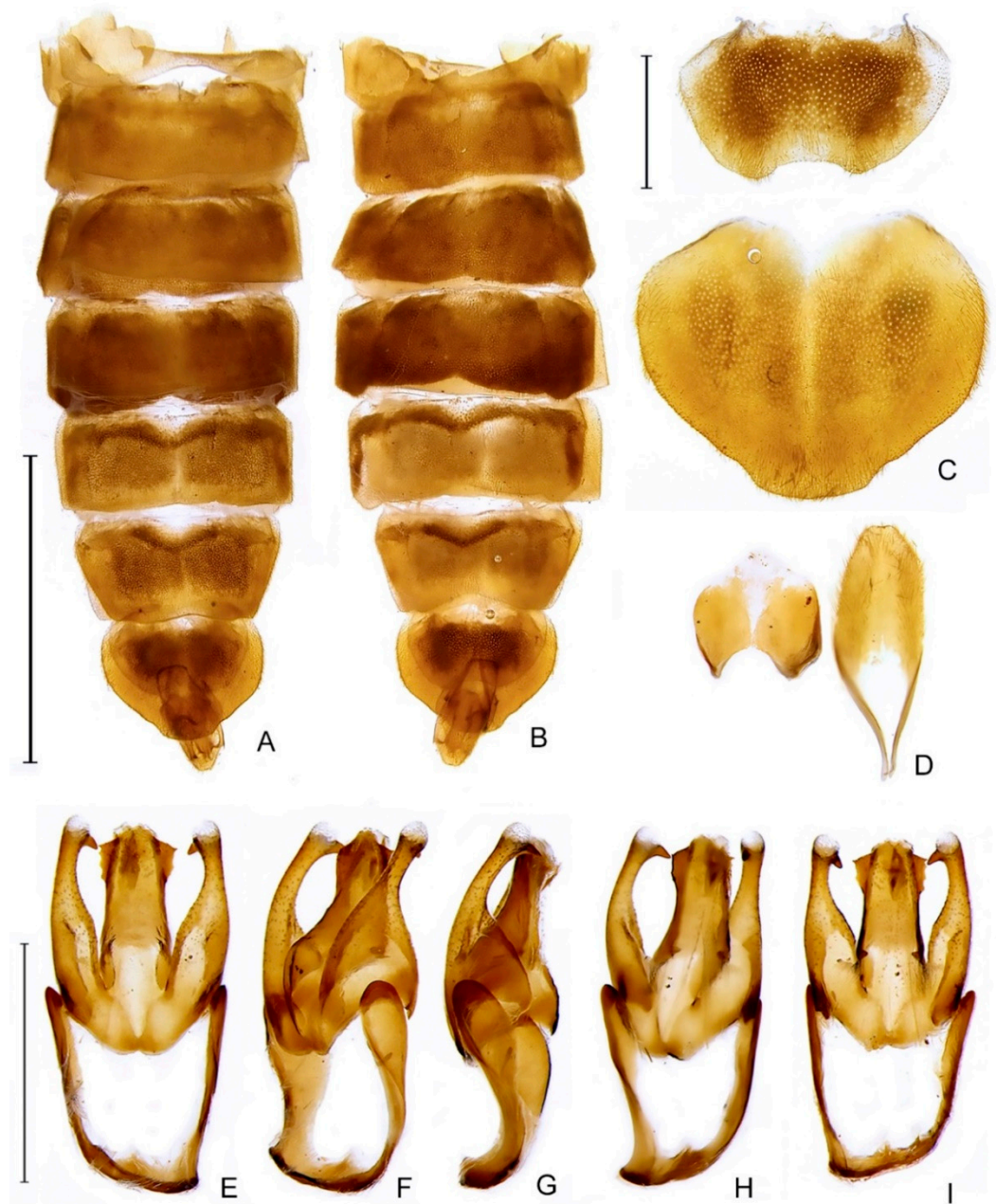


Figure 9. *Zoiudo araucariorum* sp. nov., abdomen: (A) dorsal, (B) ventral. (C) Pygidium, dorsal and sternum VIII, ventral. (D) Aedeagal sheath (syntergite, dorsal; sternum IX, ventral). (E–I) Aedeagus: (E) dorsal, (F) dorso-lateral, (G) lateral, (H) lateroventral, (I) ventral. Scale bars: (A,B): 5 mm; (C,D): 1 mm; (E–I): 1 mm.

urn:lsid:zoobank.org:act:8D57236E-C76F-4A6A-83B8-F95A3E0A0AA9

Type species. *Zoiudo rosae* sp. nov., by original designation.

Diagnosis. Head moderately depressed at vertex, antennal socket subtriangular (Figure 4D); antennae filiform, antennomeres III–X progressively shorter toward apex (Figure 4F); pronotum with posterior angle slightly projected posteriorly (Figure 5A), anterior expansion strongly convex (Figure 5A), hypomeron extremely short in lateral view (slightly longer than deep) (Figure 5E); tibial spurs absent (Figure 5N); elytra slightly dehiscent (Figure 5L); abdominal sterna VI and VII with lanterns medially constricted or split in two (Figure 3B); sternum VIII with lateral margins convergent posteriad, posterior margin truncate, not covered by VII (Figure 6C); aedeagus with phallobase asymmetrical,

dorsal plate of phallus with subapical lateral keels, with a subapical spike, parameres coplanar to phallus, with a subapical spike, with a ventral lobe (Figure 6E–I).

Etymology. “*Zoiudo*” is a Latinized form of a vernacular Portuguese word meaning “with large eyes”. Gender neutral.

Male description. Head entirely covered by pronotum when retracted (Figure 3A,B). Head capsule about $1.5\times$ wider than long, lateral margins slightly convergent posteriorly, posterior margin with two posterior parasagittal indentations (Figure 4A–E); as long as deep and moderately depressed at vertex in frontal view (Figure 4D). Eyes extremely large, slightly deeper than long in lateral view, separated from each other by about $1/3$ head width in dorsal view, almost in contact in ventral view. Antennal sockets subtriangular, as wide as distance between sockets, antennifer process indistinct (Figure 4F). Antenna 11-segmented, scape slightly constricted proximally, pedicel almost as long as wide and constricted basally, antennomeres III–X decreasing in length towards apex, filiform, without upright bristles, apical antennomere slightly longer than the subapical (Figure 4F). Frontoclypeus almost straight in frontal view (Figure 4D). Labrum connected to frontoclypeus by a membranous suture (Figure 4A); about three times wider than long, anterior margin straight or emarginate (Figure 4A). Mandibles largely overlapping, long, stout, basal $1/2$ almost straight, then evenly arcuate, apex acute, external margin sparsely setose in basal $1/2$ (Figure 4A–D). Maxilla distinctly sclerotized (Figure 4B); stipe about three times longer than wide, posterior margins truncated, palp four-segmented, palpomere III subtriangular, IV acuminate, with internal margin covered with minute, dense bristles, almost two times longer than III (Figure 4B). Labium distinctly sclerotized (Figure 4B); mentum completely divided sagittally, submentum elongated, with sides convergent posteriorly, palp three-segmented, palpomere III slightly securiform (Figure 4B). Gular sutures almost indistinct, gular bar elongate, nearly three times longer than wide, with sides biconcave (Figure 4B). Occiput piriform, as long as $1/4$ of head capsule (Figure 4E).

Thorax with pronotum subquadrangular, with posterior angle acute and slightly projected, disc subquadrate with two posterolateral impressions in dorsal view, convex in lateral view, regularly punctured, punctures small and pubescent, with a line of distinct deep marginal punctures (Figure 5A–E); pronotal expansions moderately developed, anterior expansion maximal length almost $1/2$ as long as disc, lateral expansions $1/4$ as wide as disc, posterior expansions narrow, emarginated (Figure 5A–E); slightly wider than distance between elytral humeri (Figure 3A). Hypomeron extremely short in lateral view (slightly longer than deep) (Figure 5E). Prosternum three times as wide as its major length, narrowed parasagittally (Figure 5B). Proendosternite elongated, about as long as distance between the apices of proendosternite arms (Figure 5C,D). Mesoscutellum with posterior margin subtruncate (Figure 5F). Elytron narrowed posteriorly, slightly dehiscent, almost $4.5\times$ longer than wide, pubescent, with a row of conspicuous punctures surrounding sutural and lateral margins, and with longitudinal slightly elevated costae (Figure 5L). Hind wing well-developed, posterior margin slightly straight, $\sim 2.5\times$ longer than wide, r3 slightly longer than r4, radial cell three times wider than long, almost reaching anterior margin, costal row of setae inconspicuous; CuA1, CuA2, CuA3+4, CAS, and AA4 present; MP3+4 split posterior to CuA1 insertion; AA3 elongate and at an acute angle to AA4; J indistinct (Figure 5M). Alinotum subquadrate, lateral margins slightly convergent posteriorly, posterior margin slightly sinuate, rounded area of scutum weakly sclerotized, scutum—prescutal plates sclerotized, extending ridges almost to posterior margin, metascutellum glabrous (Figure 5F); anterior margin of alinotum strongly trisinuate (Figure 5G,H). Mesosternum weakly sclerotized, blunt medially, mesepimeron attached to metasternum by membrane, mesosternum/mesepisternum suture largely obliterate, but posterior half somewhat conspicuous, mesepisternum/mesepimeron suture conspicuous (Figure 5I,J). Metasternum slightly depressed anteriorly (mesocoxal rests), anterior medial keel prominent up to anterior $1/3$, discrimen distinct by basal $1/3$, lateral margins divergent posteriorly up to lateral-most part of metacoxa, then convergent posteriorly, posterior margin bisinuate (Figure 5I–K). Profemur about as long as protibia (Figure 5N), meso and metafemora

slightly shorter than respective tibiae (Figure 5N). Tibial spur absent (Figure 5N,O). Claws lacking basal teeth (Figure 5N,O). Tarsomere I two times longer than II, II subequal (pro and mesotarsus) to two times (metatarsus) longer than III, III two times longer than IV, IV bilobed, lobes reaching $2/3$ V length (Figure 5N,O). Mesendosternum with two parasagittal projections directed outwards, irregularly alate (with flaps of irregular width) (Figure 5J). Metendosternum diamond-shaped, spatulate, $2.5\times$ longer than wide, median projection acute anteriad, with two lateral laminae (Figure 5J).

Abdomen. Tergum I with anterior margin membranous, central $1/4$ sinuose, laterotergite membranous, subsquared, with sparse bristles (Figure 6B); Terga II–VII with posterolateral angles almost right-angled (not produced, rounded), IV and V with posterior margin slightly emarginate medially (Figure 6A). Sterna II–IX visible (Figure 6B). Spiracles dorsal, at about $1/2$ sterna length (Figure 6A). Sterna VI–VII bearing transversa, ellipsoid lanterns, somewhat rounded and medially constricted, sometimes split (Figure 6B). Sternum VIII about $2/3$ as long as VII, with lateral margins convergent posteriorly, posterior margin straight, coplanar to (not covered by) VII (Figure 6C); abdominal sternum IX $2.5\times$ longer than wide, posteriorly round; around two times longer than syntergite; bristled at the posterior $1/2$; lateral margins symmetric, slightly convergent posteriorly, with posterior margin subtruncate or emarginate (Figure 6D); pygidium roughly heart-shaped, posterolateral angles obsolete, with anterior margin slightly emarginated medially, lateral margins roundly convergent posteriorly, and posterior margin rounded (Figure 6C); syntergite symmetrical or asymmetrical, with posterior margin acuminate, anterior margin emarginate; suture between abdominal terga IX and X indistinct, posterior corners bristled posteriorly; well-sclerotized except by a central irregular oblong region (Figure 6C); aedeagus with phallobase asymmetrical, dorsal plate of phallus basally fused to parameres, without subapical keel, endosac opens ventral to dorsal plate (i.e., not across the dorsal plate as in *Photinus* Laporte, 1833 spp.) with subapical lateral indentations, ventral plate rudimentary, restricted to a sclerotized piece outlining the ejaculatory duct; paramere arms subparallel, apically tapered with a subapical spike, with a basal ventral lobe (Figure 6E–I).

Coloration (Figure 3A,B). Body overall brown to dark-brown, except for: antennal scape light brown; light brown pronotal expansions, and elytral inner and outer margin (outlined in light brown, outer stripe sometimes reaching elytron mid-width); legs light brown up to basal $1/3$ of tibia, then dark brown, with brown tibia and tarsus; abdominal segments VI and VII variably translucent; pygidium light brown, often with a darker stripe at central $1/3$ to $1/4$. Sternum VIII with translucent lateral spots.

Immature stages and female. Unknown.

Distribution. The genus is known from Chapada dos Guimarães, Mato Grosso State (Cerrado Biome), and São Bento do Sul, Santa Catarina State (Araucaria Forest in Atlantic Rainforest Biome), Brazil (Figure 10). The distribution and diversity of this genus is likely underestimated due to lack of targeted sampling, at least between these two largely distant sites.

Biology. *Zoiudo rosae* sp. nov. males were collected at night using light traps (white sheet). Along with the species overall morphology, with bulgy eyes, short antennae, and the presence of lanterns, males might be following light signals from females. Given the striking similarity between the two species of *Zoiudo* gen. nov., it is likely that the *Zoiudo araucariorum* sp. nov. has a similar biology.

Remarks. *Zoiudo* gen. nov. can be distinguished from all other Photinini genera by the combination of medially constricted or split lanterns on sterna VI and VII, absence of tibial spurs, and the presence of lateral keels on the dorsal plate of phallus. Among Photinini genera, *Zoiudo* gen. nov. is morphologically similar to *Ybytyramoan*, with which it shares the large eyes, housed under pronotal bulges, pronotum without a notch on the posterior angle, sternum VIII with lateral margins convergent posteriorly, parameres with a subapical spike. However, *Zoiudo* gen. nov. has the pronotal posterior angles slightly projected (obtuse in *Ybytyramoan*), elytra dehiscent (elytra widest at the posterior $1/3$ in *Ybytyramoan*), tibial spurs absent (each leg with a pair of tibial spurs in *Ybytyramoan*), rounded and medially

constricted to completely separate and divided lanterns (rounded or billycock-shaped in *Ybytyramoan*), pygidium somewhat heart-shaped (with sides rounded in *Ybytyramoan*), dorsal plate of aedeagus without a subapical dorsal keel (present in *Ybytyramoan*), and with subapical lateral keels (absent in *Ybytyramoan*). *Zoiudo* gen. nov. is also similar to *Photinus* in outline, from which it can be easily differentiated by the absence of a pronotal notch on the posterior angle, absence of tibial spurs (tibial spur formula 1-2-2 or 2-2-2 in *Photinus*), the sternum VIII coplanar with VII (usually partially retracted under VII in *Photinus*), and the lack of phallic ventrobasal processes (present in *Photinus*).

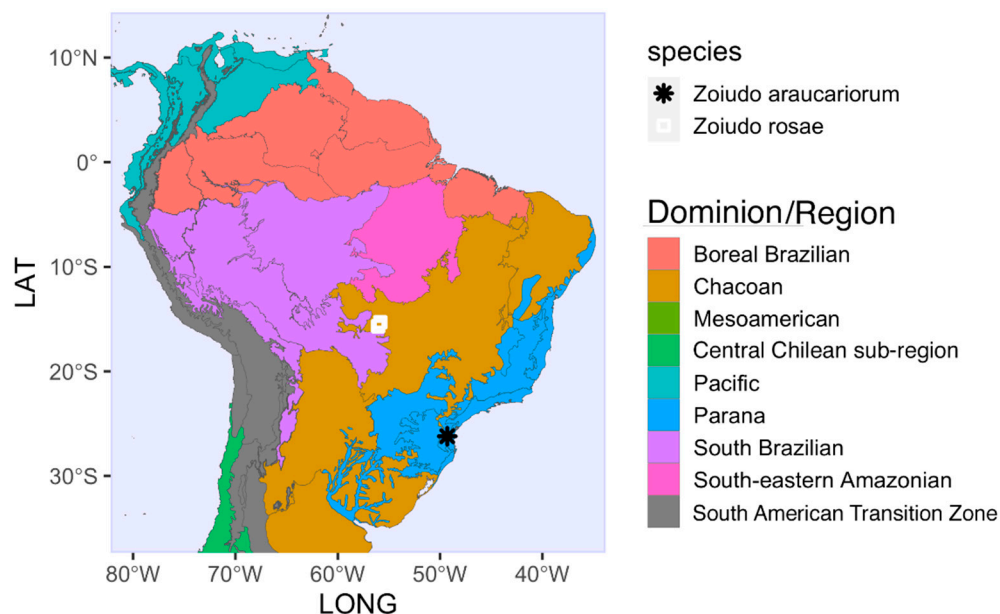


Figure 10. Distribution range of *Zoiudo* gen. nov. and its two species, on a map superimposed with the dominions as in Morrone et al., 2022.

Key to *Zoiudo* gen. nov. species

1 Body length around 18.8 mm, phallus with lateral keel of dorsal plate smooth (except for subapical spike, Figure 6E–I), surface of parameres almost smooth (with few dome-shaped sensillae), *Zoiudo rosae* sp. nov.

1' Body length around 16.5 mm, phallus with lateral keel of dorsal plate irregularly undulated, parameres covered on dome-shaped sensillae, which makes its surface look rougher (Figure 9E–I), *Zoiudo araucariorum* sp. nov.

Zoiudo rosae Roza, Mermudes and Silveira sp. nov.

(Figure 3, Figure 4, Figure 5, Figure 6)

urn:lsid:zoobank.org:act:EA686303-3D49-49A4-8DDB-58DC4B4A2B4B

Diagnostic description. Body length around 18.8 mm ($n = 5$, from 18.4 to 19.5 mm). Labrum with anterior margin straight or emarginate (Figure 4A). Sternum VIII lantern medially constricted to divided in two (Figure 3B). Phallus with lateral keel of dorsal plate smooth (except for subapical spike) (Figure 6E–I). Surface of parameres almost smooth (with very few sensillae compared to *Zoiudo araucariorum* sp. nov.; Figure 9E–I).

Etymology. “*rosae*” is a noun in the genitive case. This species is named in honor of the Brazilian entomologist Simone Policena Rosa, a leading expert on Elateroid groups, with a special emphasis on their immature stages. Simone encouraged and auxiliated us to study fireflies. She was also among the collectors of the specimens of this new species.

Remarks. The aedeagus morphology was stable on two dissected specimens collected in different expeditions.

Type material. Male Holotype: BRAZIL. Mato Grosso. “Brasil Chapada dos Guimarães-/MT Cidade de Pedra/17-24.X.2009 LUZ/S.P. Rosa, F. Fernandes,/B. Medeiros & L. Prado

col.” (MZSP). Male Paratypes: BRAZIL. Mato Grosso. Same data as holotype (5 males–DZRJ; 34 males–MZSP) (1 with body dissected); “MT. Chapada dos Guimarães/17.X.1995/Grace David” (1 male–CEMT) (abdomen dissected); “MT–Cuiabá/Faz. Nirvana/XI-1988/Miriam Serrano” (1 male–CEMT).

***Zoiudo araucariorum* Roza, Mermudes and Silveira sp. nov.**

(Figure 7, Figure 8, Figure 9, Figure 10)

urn:lsid:zoobank.org:act:3250C749-CBE8-4CE1-928A-377C58E32001

Diagnostic description. Body length around 16.5 mm (n = 1). Labrum with anterior margin truncate (Figure 7B). Sternum VIII lantern medially divided in two (Figure 7B). Phallus with lateral keel of dorsal plate irregularly undulated (Figure 9E–I). Parameres covered on dome-shaped sensillae, which makes its surface look rougher (Figure 9E–I).

Etymology. “*araucariorum*” is a noun in the genitive case, after the *Araucaria* trees, which are abundant on the type locality of this new species.

Type material. Male Holotype: BRAZIL. Santa Catarina. “BRASIL/Rio Vermelho [São Bento do Sul]/ Sta. Catarina/ VIII/63 Dirings” (MZSP) (abdomen dissected, Figure 9A–I).

4. Discussion

4.1. Phylogeny and Classification of Photinini

Our study used morphological characters to address the phylogeny of Photinini to inform the taxonomy of *Zoiudo* gen. nov. Our study found *Zoiudo* gen. nov. to be the sister of *Ybytyramoan*, with high support (see above). This node has been consistently found sister to *Lucidota banoni*, the type species of its genus. The other *Lucidota* species in our sampling, *L. atra* Olivier 1790, was recovered at another branch, consistent with the artificial definition of this genus [6].

A few other clusters are recurrent in recent phylogenies. For example, *Scissicauda* + *Haplocauda*, *Alychnus* + *Photinus*, *Costalampys* + *Dadophora*, and *Luciuranus* (*Lucidota atra* (*Phosphaenus* + *Phosphaenopterus*)) are all well-supported nodes. In contrast, the backbone of Photinini was largely unresolved or resolved without support, a recurrent pattern in published morphology-based phylogenies of the Lampyridae [4,5,7]. In addition, the finer resolution of the analyses with implied weights is sensitive to K value. The lack of resolution might suggest a relatively fast radiation of this lineage, consistent with the greater species diversity of this branch.

Even though nearly half of Photinini genera are represented in our study, the sampling within genera is still rudimentary to subsidize a comprehensive taxonomic review of this tribe. Future studies should focus on covering more taxa and morphological characters and combine with other data sources when available.

4.2. Hypothesized Habits of *Zoiudo*

Individuals of *Zoiudo* gen. nov. are yet to be observed alive. However, comparing its morphology with other known Photinini could provide insight on its biology. *Ybytyramoan*—the sister taxon of *Zoiudo* gen. nov.—is known from three nocturnal species in which males produce long single-flashes ([9], Silveira, pers. ob.), like some *Photinus* spp. [29]. However, the relatively larger eyes and shorter antennae of male *Zoiudo* gen. nov. are closer to those *Magnoculus* McDermott, 1964, *Lamprohiza* Motschulsky, 1853, and *Phausis* LeConte, 1851—rather than *Ybytyramoan*—suggesting that they might be after glows, not flashes, as courting signals [30].

5. Conclusions

Here we described two new species of Photinini, recovered as a new monophyletic genus close to *Ybytyramoan*. Our study confirms the value of extensive character and taxon sampling towards a revised classification of Photinini taxa and highlights the need for the continued sampling and protection of South American biomes before they are gone.

Supplementary Materials: The following supporting information can be downloaded at: <https://www.mdpi.com/article/10.3390/d14111005/s1>, Supplementary Material S1: additional material used in the phylogenetic analyses. Supplementary Material S2: character matrix, as simplified nexus. Supplementary Material S3: results of the model selection by ModelFinder. Supplementary Material S4: outgroups mandible morphology. Supplementary Material S5: alternative topologies recovered on the implied weighted maximum parsimony analyses.

Author Contributions: Conceptualization, A.S.R. and L.F.L.d.S.; methodology, A.S.R., J.R.M.M. and L.F.L.d.S.; formal analysis, A.S.R. and L.F.L.d.S.; investigation, A.S.R., J.R.M.M. and L.F.L.d.S.; resources, A.S.R., J.R.M.M. and L.F.L.d.S.; data curation, A.S.R., J.R.M.M. and L.F.L.d.S.; writing—original draft preparation, A.S.R. and L.F.L.d.S.; writing—review and editing, A.S.R., J.R.M.M. and L.F.L.d.S.; supervision, L.F.L.d.S.; project administration, A.S.R., J.R.M.M. and L.F.L.d.S.; funding acquisition, A.S.R., J.R.M.M. and L.F.L.d.S. All authors have read and agreed to the published version of the manuscript.

Funding: ASR was funded by CNPq fellowship 150747/2022-5, JRMM by CNPq fellowship 311679/2019-6. Several specimens included in that study were dissected under equipment funded by NSF#2001683 CSBR: Natural History: Development of the Catamount.

Data Availability Statement: Data is contained within the article and its supplementary material.

Acknowledgments: We thank Sonia Casaria (MZSP) and Fernando Vaz-de-Mello (CEMT) for lending us the material to use in this study. We thank Gabriel Biffi by sending information regarding MZSP holdings of MZSP Photinini.

Conflicts of Interest: The authors declare no conflict of interest. The funders had no role in the design of the study; in the collection, analyses, or interpretation of data; in the writing of the manuscript, or in the decision to publish the results.

References

1. Branham, M.A.; Wenzel, J.W. The origin of photic behavior and the evolution of sexual communication in fireflies (*Coleoptera: Lampyridae*). *Cladistics* **2003**, *19*, 1–22. [[CrossRef](#)] [[PubMed](#)]
2. Vaz, S.; Mermudes, J.R.M.; Paiva, P.C.; Silveira, L.F.L. Systematic review and phylogeny of the firefly genus *Dilychnia* (*Lampyridae: Lampyrinae*), with notes on geographical range. *Zool. J. Linn. Soc.* **2020**, *190*, 844–888. [[CrossRef](#)]
3. Silveira, L.F.L.; Rosa, S.P.; Mermudes, J.R. Systematic review of the firefly genus *Lucernuta* Laporte, 1833 (*Coleoptera: Lampyridae*). *Ann. Zool.* **2019**, *69*, 293–314. [[CrossRef](#)]
4. Silveira, L.F.L.; Roza, A.S.; Vaz, S.; Mermudes, J.R.M. Description and phylogenetic analysis of a new firefly genus from the Atlantic Rainforest, with five new species and new combinations (*Coleoptera: Lampyridae: Lampyrinae*). *Arthropod Syst. Phylogeny* **2021**, *79*, 115–120. [[CrossRef](#)]
5. Silveira, L.F.L.; Lima, W.; Fonseca, C.R.V.D.; McHugh, J. *Haplocauda*, a New Genus of Fireflies Endemic to the Amazon Rainforest (*Coleoptera: Lampyridae*). *Insects* **2022**, *13*, 58. [[CrossRef](#)] [[PubMed](#)]
6. McDermott, F.A. The taxonomy of the *Lampyridae* (*Coleoptera*). *Trans. Am. Entomol. Soc.* **1964**, *90*, 1–72.
7. Ladino-Peñuela, A.G.; Botero, J.P.; Silveira, L.F.L. First Phylogeny of *Pseudolychnuris* Reveals Its Polyphyly and a Staggering Case of Convergence at the Andean Paramos (*Lampyridae: Lampyrini*). *Insects* **2022**, *13*, 697. [[CrossRef](#)]
8. Kazantsev, S.V. New firefly taxa from Hispaniola and Puerto Rico (*Coleoptera: Lampyridae*), with notes on biogeography. *Russ. Entomol. J.* **2006**, *15*, 367–392. [[CrossRef](#)]
9. Silveira, L.F.L.; Mermudes, J.R.M. *Ybytyramoan*, a new genus of fireflies (*Coleoptera: Lampyridae, Lampyrinae, Photinini*) endemic to the Brazilian Atlantic Rainforest, with description of three new species. *Zootaxa* **2014**, *3835*, 325–337. [[CrossRef](#)]
10. Zaragoza-Caballero, S.; Navarrete-Heredia, J.L. Descripción de cuatro especies de *Ankonophallus* gen. nov. (*Coleoptera: Lampyridae: Photinini*). *Dugesiana* **2014**, *21*, 125–130.
11. Costa, C. Neotropical *Coleoptera*, state of knowledge. In *Hacia un Proyecto CYTED para el Inventario y Estimación de la Diversidad Entomológica en Iberoamérica: PrIBES 2000. Trabajos del 1er Taller Iberoamericano de Entomología Sistemática, Villa de Leyva, Colombia; Martín-Piera, F., Morrone, J.J., Melic, A., Eds.; Monografías Tercer Milenio: Zaragoza, Mexico, 2000; Volume 1, pp. 99–114.*
12. Mittermeier, R.A.; Turner, W.R.; Larsen, F.W.; Brooks, T.M.; Gascon, C. Global biodiversity conservation: The critical role of hotspots. In *Biodiversity hotspots*; Zachos, F., Habel, J., Eds.; Springer: Berlin/Heidelberg, Germany, 2011; pp. 3–22. [[CrossRef](#)]
13. Machado, R.B.; Ramos, M.B.N.; Pereira, P.; Caldas, E.; Gonçalves, D.; Santos, N.; Tabor, K.; Steininger, M. *Estimativas de Perda da área do Cerrado Brasileiro*; Relatório técnico não publicado; Conservação Internacional: Brasília, Brazil, 2004.
14. Martin, G.J.; Stanger-Hall, K.F.; Branham, M.A.; Silveira, L.F.L.; Lower, S.E.; Hall, D.W.; Li, X.; Lemmon, A.R.; Lemmon, E.M.; Bybee, S.M. (2019). Higher-level phylogeny and reclassification of *Lampyridae* (*Coleoptera: Elateroidea*). *Insect Syst. Divers.* **2019**, *3*, 11. [[CrossRef](#)]

15. Lawrence, J.F.; Zhou, Y.L.; Lemann, C.; Sinclair, B.; Ślipiński, A. The hind wing of *Coleoptera* (Insecta): Morphology, nomenclature and phylogenetic significance. Part 1. General discussion and Archostemata–Elateroidea. *Ann. Zool.* **2021**, *71*, 421–606. [[CrossRef](#)]
16. Morrone, J.J.; Escalante, T.; Rodríguez-Tapia, G.; Carmona, A.; Arana, M.; Mercado-Gómez, J.D. Biogeographic regionalization of the Neotropical region: New map and shapefile. *An. Da Acad. Bras. De Ciências* **2022**, *94*, e20211167. [[CrossRef](#)]
17. Sereno, P.C. Logical basis for morphological characters in phylogenetics. *Cladistics* **2007**, *23*, 565–587. [[CrossRef](#)] [[PubMed](#)]
18. Maddison, W.P.; Maddison, D.R. Mesquite Version 3.51. A Modular System for Evolutionary Analysis. Available online: <http://www.mesquiteproject.org> (accessed on 13 September 2022).
19. Goloboff, P.A.; Farris, J.S.; Nixon, K.C. TNT, a free program for phylogenetic analysis. *Cladistics* **2008**, *24*, 774–786. [[CrossRef](#)]
20. Goloboff, P.A.; Carpenter, J.M.; Arias, J.S.; Esquivel, D.R.M. Weighting against homoplasy improves phylogenetic analysis of morphological data sets. *Cladistics* **2008**, *24*, 758–773. [[CrossRef](#)]
21. Marcos Mirande, J. Weighted parsimony phylogeny of the family Characidae (*Teleostei: Characiformes*). *Cladistics* **2009**, *25*, 574–613. [[CrossRef](#)]
22. Huelsenbeck, J.P.; Ronquist, F. MRBAYES: Bayesian inference of phylogenetic trees. *Bioinformatics* **2001**, *17*, 754–755. [[CrossRef](#)] [[PubMed](#)]
23. Miller, M.A.; Pfeiffer, W.; Schwartz, T. The CIPRES science gateway: Enabling high-impact science for phylogenetics researchers with limited resources. In Proceedings of the 1st Conference of the Extreme Science and Engineering Discovery Environment: Bridging from the extreme to the campus and beyond, Chicago, IL, USA; 2012; pp. 1–8.
24. Kalyaanamoorthy, S.; Minh, B.Q.; Wong, T.K.; Von Haeseler, A.; Jermin, L.S. ModelFinder: Fast model selection for accurate phylogenetic estimates. *Nat. Methods* **2017**, *14*, 587–589. [[CrossRef](#)]
25. Minh, B.Q.; Schmidt, H.A.; Chernomor, O.; Schrempf, D.; Woodhams, M.D.; Von Haeseler, A.; Lanfear, R. IQ-TREE 2: New models and efficient methods for phylogenetic inference in the genomic era. *Mol. Biol. Evol.* **2020**, *37*, 1530–1534. [[CrossRef](#)]
26. Lewis, P.O. A likelihood approach to estimating phylogeny from discrete morphological character data. *Syst. Biol.* **2001**, *50*, 913–925. [[CrossRef](#)] [[PubMed](#)]
27. Rambaut, A.; Drummond, A.J.; Xie, D.; Baele, G.; Suchard, M.A. Posterior summarisation in Bayesian phylogenetics using Tracer 1.7. *Syst. Biol.* **2018**, *67*, 901–904. [[CrossRef](#)] [[PubMed](#)]
28. Nixon, K.C. WinClada, Version 1.00. 08. Published by the Author, Ithaca, NY, 734, 745. Available online: <http://www.diversityoflife.org/winclada/> (accessed on 13 September 2022).
29. Stanger-Hall, K.F.; Lloyd, J.E. Flash signal evolution in *Photinus* fireflies: Character displacement and signal exploitation in a visual communication system. *Evolution* **2015**, *69*, 666–682. [[CrossRef](#)] [[PubMed](#)]
30. Stanger-Hall, K.F.; Sander Lower, S.E.; Lindberg, L.; Hopkins, A.; Pallansch, J.; Hall, D.W. The evolution of sexual signal modes and associated sensor morphology in fireflies (*Lampyridae, Coleoptera*). *Proc. R. Soc. B Biol. Sci.* **2018**, *285*, 20172384. [[CrossRef](#)] [[PubMed](#)]